DOI: 10.1002/ejoc.200800335

Photoinduced Electron Transfer in Branched Bis(ferrocenylacetylene)-C_{60} Systems: Influence of the Nature of Conjugation

Laura Pérez,[a] D.-M. Shafiqul Islam,[b,c] Yasuyuki Araki,[b] Pilar de la Cruz,[a] François Cardinali,[a] Osamu Ito,*[b] and Fernando Langa*[a]

Keywords: Fullerenes / Electron transfer / Metallocenes

Four new branched 3,4- and 3,5-bis(ferrocenylacetylene)-phenyl-C_{60} molcules, in which the bis-ferrocene donor moieties and C_{60} acceptor moiety are covalently linked with phenylacetylene linkage through pyrrolidino and pyrazolino rings on the C_{60} moiety, as abbreviated to be $(Fc)_2$≡Ph-NMPC_{60} (*o*- and *m*-) and $(Fc)_2$≡Ph-PzC_{60} (*o*- and *m*-), respectively, have been prepared in multistep procedures using microwave irradiation, as source of energy. The HOMO–LUMO gaps smaller than 1.25 eV were experimentally determined by cyclic voltammetry (CV) and Osteryoung square-wave voltammetry (OSWV) for $(Fc)_2$≡Ph-PzC_{60} and $(Fc)_2$≡Ph-NMPC_{60}. In both polar and non-polar solvents, a photoinduced charge-separation (CS) process efficiently takes place in $(Fc)_2$≡Ph-NMPC_{60} and $(Fc)_2$≡Ph-PzC_{60} from the singlet excited state of C_{60} ($^1C_{60}^*$), as confirmed by picosecond-time-resolved emission spectroscopy. The CS states were confirmed by nanosecond-transient absorption spectroscopy. The lifetimes of the CS states were evaluated to be ca. 10 ns, which are shorter than those of the similar dyads with phenylenevinylene linkage, suggesting higher electron-hole conductivity through the phenylacetylene linkage.

Introduction

A topic of high interest in terms of artificial photosynthesis and optoelectronic devices concerns π systems having electron-acceptor ability substituted with electron-donor groups.[1] In many of such assemblies, C_{60} has been proven to be a good electron-acceptor due to the spherically delocalized π-electron system accompanying by its interesting electrochemical and electronic properties[2] and has been combined with many electron-donors including porphyrins,[3] phthalocyanines,[4] transition metal complexes,[5] TTF[6] or ferrocene. Ferrocene is particularly appealing as donor because ferrocene combines chemical versatility with high thermal stability. Moreover, several examples of efficient photoinduced electron transfer in ferrocene–fullerene systems have been reported confirming that ferrocene is an excellent electron donor.[7]

One important point is to enhance the light-harvesting ability of the molecules, in which an array of branched electron-donors, acting as peripheral chromophores, transfers the collected energy to a fullerene C_{60} core, as have recently been reported by several groups.[8] We have recently described the synthesis of new branched systems with ferrocene units on their periphery where phenylvinylene (PV) bridges connected the ferrocenes to a pyrrolidinofullerene $(Fc)_2$ = Ph–NMPC_{60} **1** (Scheme 1).[9] The nanosecond transient absorption spectral studies revealed efficient photoinduced charge separation even in toluene as solvent, which is prospective for wide applications in non-polar media such as polymer films. Interestingly, when the same donor moiety

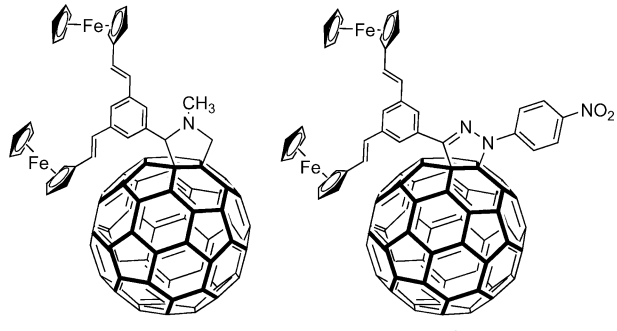

Scheme 1. Reference fullerene derivatives **1** and **2**.

[a] Facultad de Ciencias del Medio Ambiente, Universidad de Castilla-La Mancha,
45071 Toledo, Spain
Fax: +34-925-268-840
E-mail: Fernando.LPuente@uclm.es
[b] Institute of Multidisciplinary Research for Advanced Materials, Tohoku University,
Katahira, Sendai 980-8577, Japan
E-mail: ito@tagen.tohoku.ac.jp
[c] Department of Chemistry, Graduate School of Science, Jahangirnagar University,
Savar, Dhaka 1342, Bangladesh

Supporting information for this article is available on the WWW under http://www.eurjoc.org or from the author.

is connected to a pyrazolinofullerene $(Fc)_2$ = Ph–PzC_{60} **2** (Scheme 1) the lifetime of the radical ion pair is three times longer.[10]

It has been expected that the nature of the central π-bridges can significantly affect the electron-hole transfer rates in addition to the electronic and photophysical properties on ferrocene and C_{60},[11] but the effects caused by the conjugation pattern of the π-bridges are far from being understood. Most attention has been so far devoted to the PV bridges[12] but phenylacetylene (PA) units have only recently received some interests as highly conductive molecular wire.[13]

As a part of these researches, we now report the synthesis of several C_{60} derivatives bearing 3,4- and 3,5-bis(ferrocenylacetylene)phenyl moieties as a donor-bridge set where the donor-bridge unit and the fullerene are linked by both pyrrolidino [$(Fc)_2$≡Ph–$NMPC_{60}$, **4a**,**b**] and pyrazolino ring [$(Fc)_2$≡Ph–PzC_{60}, **6a**,**b**] via a phenyl group as shown in Scheme 2.

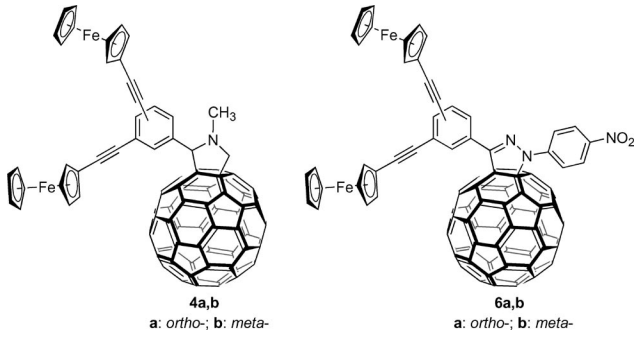

Scheme 2. New branched bis(ferrocenylacetylene)-C_{60} systems (**4a**,**b** and **6a**,**b**).

Results and Discussion

Synthesis

The preparation of the bis(ferrocenylacetylene)benzaldehydes **3a**,**b** is depicted in Scheme 3. Afterwards, the formed *Z*/*E* isomers mixture reacted with *n*-butyllithium according to a modification of the reported procedure.[14] Compounds **3a**,**b** were prepared by the palladium-catalyzed Sonogashira alkynylation reaction[15] of acetyleneferrocene with 3,4- and 3,5-dibromobenzaldehyde using $PdCl_2(PPh_3)_2$/CuI as catalyst and triethylamine as solvent. These reactions require long reaction times, and microwave irradiation has shown to be very efficient in Sonogashira coupling reactions;[16] accordingly, the synthesis of **3a**, using a standard CEM Discover microwave reactor (200 W, 1.5 h), was performed[17] to give **3a** in 93% yield. Using analogous conditions (200 W, 2 h), **3b** was prepared in 98% yield.

The target pyrrolidinofullerenes **4a**,**b** were prepared by 1,3-dipolar cycloaddition of the aldehydes **3a**,**b**, *N*-methylglycine and C_{60} according to the Prato method[18] in toluene

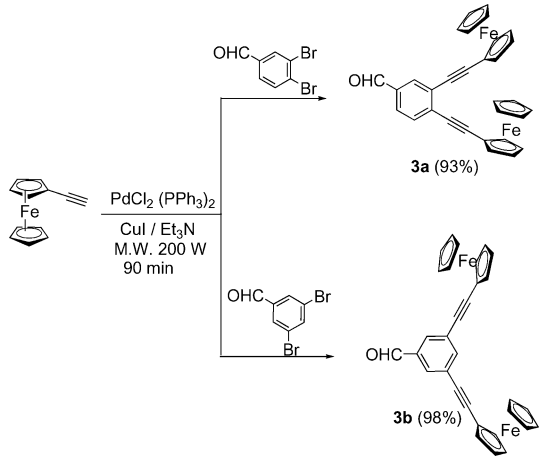

Scheme 3. Synthesis of aldehydes **3a**,**b**.

(reaction time 5–8 h) in 36% and 37% yield, respectively. The effectiveness of microwave irradiation in cycloaddition reactions[19] and in fullerene chemistry[20] has been widely documented and by using this technique (CEM Discover, 200 W, reaction time 1.5 and 2 h in that order) **4a**,**b** were obtained in 39% and 41% yield, respectively (Scheme 4).

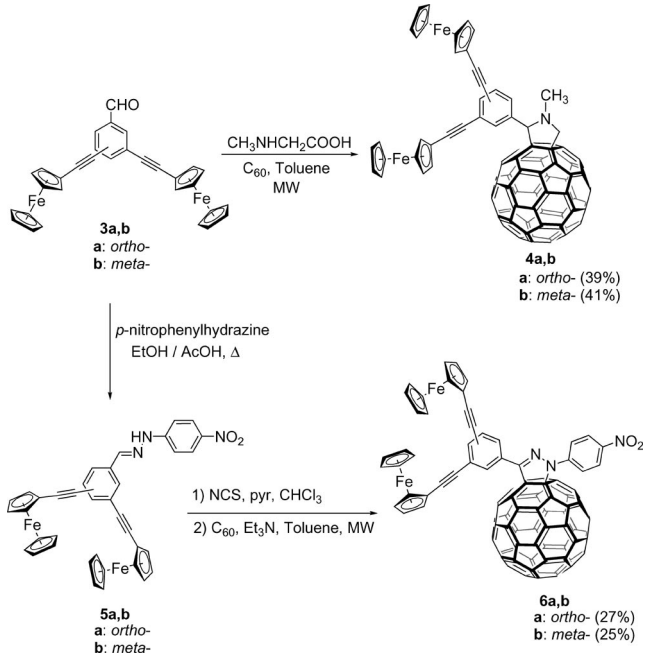

Scheme 4. Synthesis of $(Fc)_2$≡Ph–$NMPC_{60}$ (**4a**,**b**) and $(Fc)_2$≡Ph–PzC_{60} (**6a**,**b**) systems.

Finally, to prepare the goal pyrazolinofullerenes **6a**,**b** (Scheme 2), it was necessary to obtain the intermediate hydrazones **5a**,**b** by reaction of aldehydes **3a**,**b** with 4-nitrophenylhydrazine in refluxing ethanol (yields 83% and 90%, respectively). Treatment of hydrazones **5a**,**b** with *N*-chlorosuccinimide (NCS) and pyridine in $CHCl_3$ at 0 °C,

followed by reaction with triethylamine afforded the intermediate nitrile imines which were reacted in situ, by 1,3-dipolar cycloaddition,[21] with C_{60} under microwave irradiation at 200 W (1.0–1.5 h). Compounds **6a**,**b** were obtained in 27% and 25% yield, respectively, after purification by column chromatography.

The structures of fullerene derivatives **4a**,**b** and **6a**,**b** were confirmed by their analytical and spectroscopic data (UV/Vis, FTIR, ^{1}H NMR, ^{13}C NMR and MALDI mass spectra) although the low solubility of compounds **6a**,**b** prevented to record the ^{13}C spectra with good quality. The ^{1}H NMR spectra are consistent with the proposed structures. As a representative example, the presence of the ferrocene moiety is revealed by the signals between δ = 4.2 and 4.6 ppm, and the fingerprint of the pyrrolidine ring appears as two doublets and one singlet between δ = 4.3 and 5.0 ppm. In fulleropyrrolidines **4a**,**b**, the signals of the *ortho*-hydrogen atoms of the phenyl group contiguous to the pyrrolidine ring appear as broad signals at room temperature due to the known free rotation of the phenyl group in phenylpyrrolidinofullerenes.[22] This effect was not observed in pyrazolines **6a**,**b** due to the conjugation of the phenyl group with the C=N group of the pyrazoline ring. The structures of **4a**,**b** were also confirmed by their MALDI-TOF mass spectra which show the expected M^+ peak at m/z = 1269.0 (**4a**,**b**) and m/z = 1375.14 (**6a**,**b**) matching the calculated molecular weights.

Electrochemical Measurements

The electrochemical properties of fullerene derivatives **4a**,**b** and **6a**,**b** were examined using cyclic voltammetry (CV) and Osteryoung square-wave voltammetry (OSWV) at room temperature in *o*-DCB/CH_3CN (4:1 v/v) as a solvent with nBu$_4$NClO$_4$ as a supporting electrolyte. The redox potentials measured by OSWV vs. Ag/$AgNO_3$ with a scan rate at 100 mV s^{-1} are collected in Table 1.

Table 1. Redox potentials (in V) of compounds **4a**,**b**, **6a**,**b**, C_{60} and ferrocene determined by OSWV[a] and free-energy changes for charge recombination (ΔG_{CR}, in eV) and charge separation via $^1C_{60}$* (ΔG^S_{CS} in eV).

	E^1_{ox}	E^1_{red}	E^3_{red}	E^3_{red}
C_{60}	–	–0.97	–1.39	–1.87
Fc	+0.09	–	–	–
4a	+0.07	–1.14	–1.53	–2.06
4b	+0.12	–1.12	–1.51	–2.11
6a	+0.02	–0.96	–1.53 (–1.78)[b]	–2.13
6b	+0.01	–0.97	–1.47 (–1.80)[b]	–2.04

[a] Experimental conditions: V vs. Ag/$AgNO_3$; glassy carbon electrode as a working electrode; 0.1 M nBu$_4$NClO$_4$; scan rate: 100 mV s^{-1}. Measured in *o*-DCB/CH_3CN (4:1 v/v) at room temperature. [b] Correspond to the irreversible reduction of the nitro group.

As representative example, the cyclic voltammogram for **4b** is shown in Figure 1, in which a reversible sharp peak appears in the positive potential, whereas, three reversible sharp peaks appear in the negative potential region up to –2.5 V.

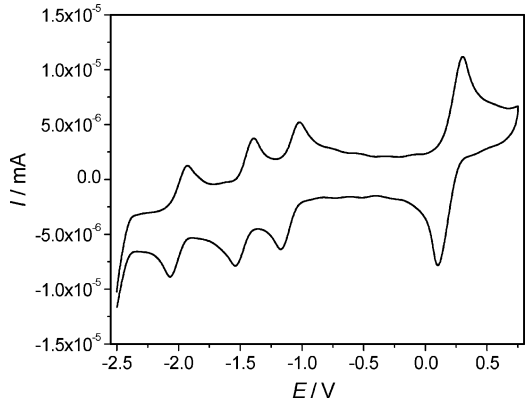

Figure 1. Cyclic voltammogram of compound **4b** in *o*-DCB/CH_3CN (4:1 v/v) (*o*-DCB = *o*-dichlorobenzene); potential (V) vs. Ag/$AgNO_3$ in the presence of nBu$_4$NClO$_4$.

As a general feature, **4a**,**b** and **6a**,**b** gave rise, in the observation window, to three reversible one-electron reduction waves in the cathodic region; these are attributed to the first three reduction potentials (E^n_{red}) of the C_{60} cage. In **6a**,**b**, another irreversible reduction wave between the second and the third reduction potentials of the C_{60} cage (as a shoulder in a case of **6a**) was observed; this is assigned to the *p*-nitrophenyl group by comparison with related compounds.[23] It should be remarked that the first reduction potential of **6a**,**b** shows an anodic shift relative to **4a**,**b**, as observed previously for other Pz-based derivatives due to the –*I* effect of the N atom directly linked to the C_{60} cage.[24] In the anodic region, a reversible oxidation process (E^1_{ox}) was observed corresponding to the ferrocene moiety.

Based on the electrochemical data, the HOMO–LUMO gap, which is defined as a difference between the E^1_{ox} value and the E^1_{red} value, was evaluated to be 1.0–1.25 eV, which is approximately corresponding to the energy of the radical ion pair. From the assignments of E^1_{ox} to Fc moiety and E^1_{red} to the C_{60} cage, radical cation is located on the Fc moiety and radical anion is located on the C_{60} cage in the most stable radical ion pair. The free-energy changes for charge recombination (ΔG_{CR}) were evaluated from the HOMO–LUMO gap with considering the electrostatic terms. The free-energy changes of charge separation (ΔG^S_{CS}) via $^1C_{60}$* were calculated as difference between the excited energy of the C_{60} cage and ΔG_{CR} as added to Table 2. Comparing **4** with **6**, the ΔG_{CR} values of **6** are less negative, suggesting the stable radical ion pair of **6** due to the pyrazoline ring effect. Compared **a** with **b**, the position of the $(Fc)_2{\equiv}Ph$– slightly affects the E^1_{ox} values: 50 mV shift for **4a**→**4b**, but –10 mV shift for **6a**→**6b**.

Compared with the PV bridge dyads (**1** and **2**), the ΔG_{CR} values of **4** and **6** in PhCN are more negative suggesting that the PV bridge stabilizes the radical ion pair more than phenylacetylene (PA) bridge does.

Table 2. Free energy changes for charge recombination (ΔG_{CR}, in eV) and charge-separation via $^1C_{60}$* (ΔG^S_{CS} in eV).

	Solvent	$-\Delta G_{CR}$	$-\Delta G^S_{CS}$[a]
4a	PhCN	1.18	0.54
	toluene	1.63	0.09
4b	PhCN	1.21	0.51
	toluene	1.66	0.06
6a	PhCN	0.94	0.76
	toluene	1.54	0.16
6b	PhCN	0.94	0.76
	toluene	1.55	0.15

[a] The $-\Delta G^S_{CS}$ values were calculated according to equations; $-\Delta G^S_{CS} = \Delta E_{00} - e\,(E_{ox} + E_{red}) - \Delta G_S$; where ΔE_{00} is the 0–0 transition energy (1.70 eV for $^1C_{60}$*). ΔG_S refers to the static energy calculated according to $-\Delta G_S = -[e^2/(4\pi\varepsilon_0)]$ ($\{1/(2R_+) + 1/(2R_-) - (1/R_{CC})/\varepsilon_S - [1/(2R_+) + 1/(2R_-)]/\varepsilon_R\}$), where ε_R and ε_S refer to solvent dielectric constants for electrochemistry and electron-transfer, respectively. R_+ and R_- are radii of the radical cation and radical anion; they are 7.2 and 4.2 Å for **4a**,**b** and 7.4 and 4.2 Å for **6a**,**b**, respectively, as cited from the optimized structures of **1** and **2** (see Supporting Information, Figure S25). R_{CC} is center-to-center distance estimated to be 15.0 Å for **4a**,**b** and, 16.0 Å for **6a** and 16.5 Å for **6b**, respectively.

Steady-State Absorption Spectra

Figure 2 shows absorption spectra of compounds **4a**,**b** and **6a**,**b** in dichloromethane. These compounds exhibit the huge absorption bands in the UV region (near 255 and 300 nm), in addition to broad weak absorption in the Vis region. For **4a**,**b**, sharp peaks at 430 nm are characteristic of fulleropyrrodine moiety, in addition 700 nm peaks appeared. In the case of **6a**,**b**, stronger broad absorption bands in the 350–450 nm region suggest the stronger interaction of π-system of C_{60} moiety and pyrazoline ring.

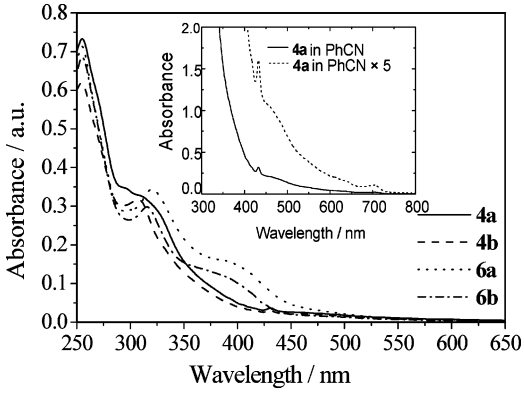

Figure 2. Steady-state absorption spectra of compounds **4a**,**b** and **6a**,**b** in CH_2Cl_2 (5×10^{-6} M). Inset: magnified steady-state absorption spectra of **4a** (5×10^{-5} M) in PhCN.

Steady-State Fluorescence Measurement

Figure 3 (top) shows the steady-state fluorescence spectra of **4a**,**b** and $NMPC_{60}$, in which the fluorescence peak at 715 nm was attributed due to the C_{60} moiety. The fluorescence intensity of **4a**,**b** in toluene was found to be decreased very much compared with that of $NMPC_{60}$, when the absorbance at the excitation wavelength (430 nm) was matched. In polar solvents such as PhCN, the fluorescence intensity of **4a**,**b** was also found to be quenched more markedly compared with that in toluene, supporting the charge-separation process via the $^1C_{60}$* is more efficient in polar solvent. For **6a**–**b** (Figure 3, bottom), appreciable fluorescence quenching of the moiety was observed in toluene compared with PzC_{60}; in PhCN, almost complete quenching was observed, which supports the efficient charge-separation process via the $^1C_{60}$* moiety in polar solvent.

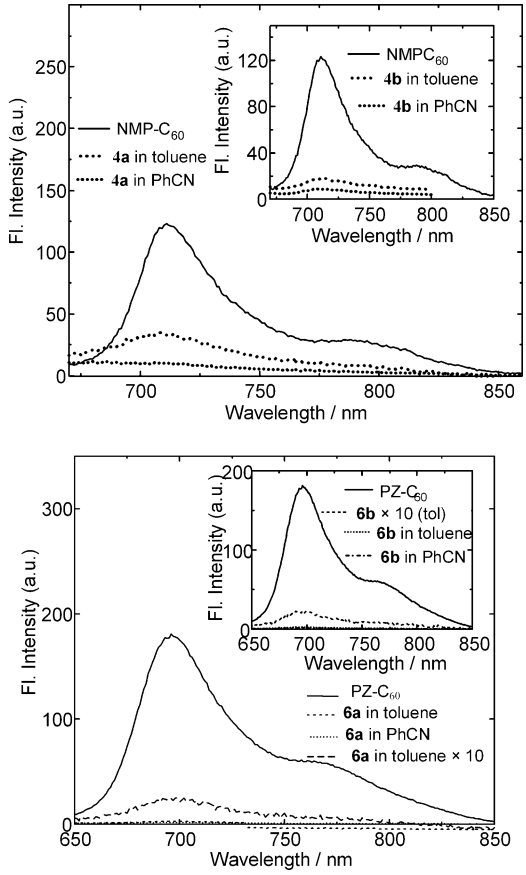

Figure 3. Steady-state fluorescence spectra of (top) **4a** (inset **4b**) and (bottom) **6a** (inset **6b**) in toluene and PhCN with the corresponding reference compounds, $NMPC_{60}$ and PzC_{60} in toluene; λ_{ex} = 430 nm.

Picosecond Fluorescence Time-Profile Measurements

The fluorescence time-profiles of **4a** and $NMPC_{60}$ are shown in Figure 4, which indicates that the fluorescence decay of the $^1C_{60}$* moiety is faster in **4a** compared with that in $NMPC_{60}$. The fluorescence time-profile decays with bi-exponential function with lifetimes [$(\tau_f)_{sample}$] as 233 ps (74%) and 1300 ps (26%) in toluene. The shortening of the fluorescence lifetime compared with $NMPC_{60}$ [$(\tau_f)_{ref}$ = 1300 ps] indicates charge separation from the Fc donor moieties to the C_{60} moiety in **4a**. A minor fraction with

lifetime same as $NMPC_{60}$ was attributed to the dissociated C_{60} derivatives, probably generated by the laser light irradiation during the lifetime measurements. In PhCN, a similar fluorescence time profile was observed, from which $(\tau_f)_{sample}$ was evaluated to be 160 ps, indicating faster charge separation (CS) in a polar solvent. For other compounds, for instance **4b** and **6a**,**b**, the evaluated $(\tau_f)_{sample}$ are summarized in Table 3.

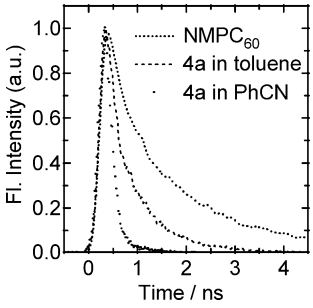

Figure 4. Fluorescence decays at 680–740 nm for **4a** in toluene and PhCN and the reference compound $NMPC_{60}$ in toluene; λ_{ex} = 400 nm.

Table 3. Fluorescence lifetimes (τ_f)[a] of $^1C_{60}$*, rate constants (k^S_{CS}) and quantum yields (Φ^S_{CS}) of charge-separation via $^1C_{60}$* of **4a**,**b** and **6a**,**b**.

Compound	Solvent	τ_f/ps (fraction)	k^S_{CS}/s^{-1}	Φ^S_{CS}
4a	toluene	233 (74%)	3.6×10^9	0.83
	PhCN	164 (78%)	6.4×10^9	0.88
4b	toluene	180 (80%)	4.8×10^9	0.86
	PhCN	132 (82%)	6.9×10^9	0.90
6a	toluene	195 (83%)	4.5×10^9	0.87
	PhCN	68 (87%)	1.4×10^{10}	0.95
6b	toluene	78 (88%)	1.2×10^{10}	0.94
	PhCN	48 (90%)	2.0×10^{10}	0.96

[a] Goodness-of-fit parameters (χ^2) were 1.00–1.17.

The charge-separation rate (k^S_{CS}) and quantum yield (Φ^S_{CS}) via the $^1C_{60}$* moiety were evaluated from the short $(\tau_f)_{sample}$ components of **4a**,**b** and **6a**,**b** according to Equations (1) and (2):[3d,7c]

$$k^S_{CS} = (1/\tau_f)_{sample} - (1/\tau_f)_{ref} \quad (1)$$

$$\Phi^S_{CS} = [(1/\tau_f)_{sample} - (1/\tau_f)_{ref}]/(1/\tau_f)_{sample} \quad (2)$$

The calculated values are listed in Table 3; for example, the k^S_{CS} and Φ^S_{CS} for **4a** were found to be 6.4×10^9 s^{-1} and 0.88 in PhCN, respectively, which indicates the occurrence of more efficient charge separation than that in toluene ($k^S_{CS} = 3.6\times10^9$ s^{-1} and Φ^S_{CS} = 0.83). For **4b**, slightly more efficient charge separation was proved compared with **4a** in both solvents. Furthermore, the charge separation process for **6a**,**b** is rapid and efficient more than **4a**–**b** in both polar solvents and non-polar solvents, indicating that the Pz moiety enhances the charge separation ability compared with the NMP moiety. For both, **4a**,**b** and **6a**,**b**, the *meta* derivatives (**b**) show more efficient charge-separation than the *ortho* derivatives (**a**) do, which can be attributed to the conformational reasons, because thermodynamic properties are the same. Furthermore, the solvent polarity affects to increase the k^S_{CS} and Φ^S_{CS} values.

From the negative ΔG^S_{CS} values listed in Table 1, the observed charge-separation processes via $^1C_{60}$* for both **4a**,**b** and **6a**,**b** are exothermic in polar solvent; i.e., the more negative ΔG^S_{CS} values for **6a**,**b** indicate that the charge-separation process is more favourable in **6a**,**b** than in **4a**,**b**. The ΔG^S_{CS} values in the range of –0.5 – –0.9 eV in PhCN suggest that the charge-separation process is almost the top region of the Marcus parabola,[25] because the reorganization energies for the C_{60} derivatives are reported to be 0.5–0.6 eV.[26] In toluene, although it is difficult to evaluate the ΔG^S_{CS} values, the observed efficient fluorescence quenching of the $^1C_{60}$* moiety suggests that the ΔG^S_{CS} values are negative even in nonpolar solvent for all **4a**,**b**, which is more negative than for **6a**,**b**. The ΔG^S_{CS} values are in the range of ca. –0.2 eV in toluene suggesting that the charge-separation process is at the foot of the normal region of the Marcus parabola.

On comparing with Fc–C_{60} dyads with the phenylvinyl (PV) linkage, the charge-separation efficiencies of phenylacetylene (PA) linkage are almost the same, suggesting that both linkages are similar molecular bridge for the charge-separation process via the $^1C_{60}$* moiety.[10]

Nanosecond Transient Absorption Studies

Nanosecond transient spectra of **4b** observed with 532 nm laser light excitation in deaerated toluene are shown in Figure 5. Immediately after the laser light pulse (6 ns), the transient absorption bands were observed at 700 nm and 1000 nm; the former band persisting longer than a microsecond was attributed to the $^3C_{60}$* moiety, whereas the latter band at 1000 nm was assigned to the $C_{60}^{\bullet-}$ moiety decaying quickly within 25 ns. Although the transient absorption band of $Fc^{\bullet+}$ was not found in Figure 5 because of weak absorbance due to the small molar absorption coefficients, the radical ion pair like as $(Fc)_2^{\bullet+}\equiv Ph–PzC_{60}^{\bullet-}$ can be presumed to be generated. From the curve-fitting with a single exponential function, the first-order rate constant was evaluated to be ca. 1×10^8 s^{-1}, which can be attributed the charge-recombination rate constant (k_{CR}). In polar PhCN, on the other hand, a more rapid decay within the 6 ns laser pulse duration was observed, suggesting $k_{CR} > 1\times10^8$ s^{-1}. For other **4a** and **6a**,**b**, rapid decays within the 6 ns laser pulse were observed, suggesting $k_{CR} > 1\times10^8$ s^{-1} in toluene and PhCN.

These lifetimes of the charge-separated states of the Fc–C_{60} dyads with the phenylacetylene (PA) linkage are quite shorter than those of the phenylvinylene (PV) linkage, suggesting that the phenylacetylene (PA) linkage is better molecular conducting wire for charge-recombination of electron-hole pair on the C_{60} and Fc, respectively.

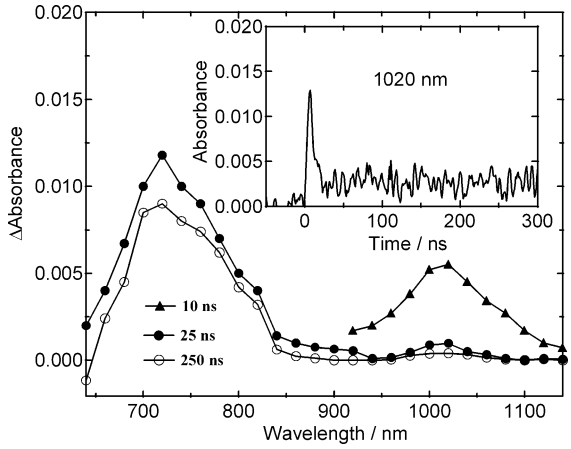

Figure 5. Transient absorption spectra obtained by 532 nm laser light photolysis of **4b** in Ar-saturated toluene.

Energy Diagram

From Table 1, the energy diagram can be schematically illustrated as shown in Figure 6. From the $(Fc)_2$≡Ph–NMP^1C_{60}* and $(Fc)_2$≡Ph–Pz^1C_{60}*, the exothermic charge separation is possible to generate $(Fc)_2^{\cdot+}$≡Ph–$NMPC_{60}^{\cdot-}$ and $(Fc)_2^{\cdot+}$≡Ph–$PzC_{60}^{\cdot-}$ in toluene and PhCN. Since the energy level of $(Fc)_2^{\cdot+}$≡Ph–$NMPC_{60}^{\cdot-}$ in toluene is higher than the triplet state $(Fc)_2$≡Ph–NMP^3C_{60}*, rapid charge recombination is anticipated. On the other hand, the energy level of $(Fc)_2^{\cdot}$≡Ph–$PzC_{60}^{\cdot-}$ in toluene is only slightly higher than $(Fc)_2$≡Ph–Pz^3C_{60}*, charge recombination goes to the lower triplet state $^3(Fc)_2$*≡Ph–PzC_{60}[27] which may be at the foot of the normal region of the Marcus parabola, which anticipates the slower charge-recombination than those for $(Fc)_2^{\cdot+}$≡Ph–$NMPC_{60}^{\cdot-}$.

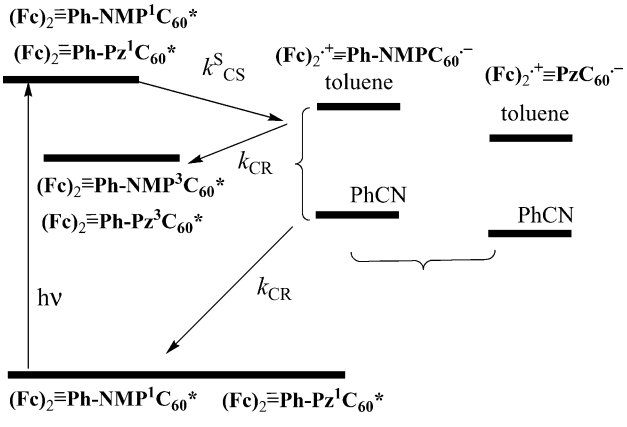

Figure 6. Energy diagram.

Conclusions

For four newly synthesized 3,4- and 3,5-bis(ferrocenylacetylene)phenyl-C_{60} systems in which the ferrocene and C_{60} are covalently linked with acetylene linkage through pyrrolidino and pyrazolino rings on the C_{60} moiety, $(Fc)_2$≡Ph–$NMPC_{60}$ (*o*- and *m*-) and $(Fc)_2$≡Ph–PzC_{60}, photoinduced charge-separation processes via the singlet excited state of C_{60} ($^1C_{60}$*) were confirmed from the fluorescence quenching measurements, which was further confirmed by the transient absorption spectra. Compared with $(Fc)_2$≡Ph–$NMPC_{60}$ (**4a**,**b**), $(Fc)_2$≡Ph–PzC_{60} (**6a**,**b**) are higher efficient charge-separation. The lifetimes of the charge-separated states of the phenylacetylene bridge systems were evaluated to be ca. 10 ns, which is shorter than those of $(Fc)_2$ = Ph–$NMPC_{60}$ and $(Fc)_2$ = Ph–PzC_{60}, probably because of higher electron-hole conductivity of the acetylene bridge than the vinylene bridge.

Experimental Section

General Remarks: C_{60} (99.9%) was purchased from MER Corporation (Tucson, AZ). Microwave irradiations were performed in a Microwave Synthesis workstation (CEM). ^{1}H NMR and ^{13}C NMR spectra were recorded on a Varian Mercury 200 and a Varian Inova 500 spectrometers. FT-IR spectra were recorded on a Nicolet Impact 410 spectrophotometer using KBr disks. MALDI-TOF mass spectra were obtained on an Applied Biosystems Voyager-DE™ STR spectrometer.

Measurements. Electrochemical Measurements: Reduction potentials E^n_{red} and oxidation potentials E^n_{ox} were measured by cyclic voltammetry (CV) and Osteryoung square wave voltammetry (OSWV) with a potentiostat BAS CV50W in a conventional three-electrode cell equipped with Pt-working and counter-electrodes with an $Ag/AgNO_3$ reference electrode at scan rate of 100 mV/s. The E_{red} and E_{ox} were expressed vs. $Ag/AgNO_3$. In each case, a solution containing 0.2 mM of a sample with 0.05 M of n-Bu_4NClO_4 (Fluka, purest quality) was deaerated with argon bubbling before measurements.

Steady-State Measurements: Steady-state absorption spectra in the visible and near-IR regions were measured on a JASCO V570 DS spectrophotometer. Steady-state fluorescence spectra were measured on a Shimadzu RF-5300 PC spectrofluorophotometer equipped with photomultiplier tube having high sensitivity in the 700–800 nm region.

Time-Resolved Fluorescence Measurements: The time-resolved fluorescence spectra were measured by the single-photon counting method using a streak-scope (Hamamatsu Photonics, C4334-01) as a detector and the laser light second harmonic generation SHG, 400 nm of a Ti:sapphire laser (Spectra-Physics, Tsunami 3950-L2S, fwhm = 1.5 ps) as an excitation source. Lifetimes were evaluated with software provided with the equipment.

Nanosecond Transient Absorption Measurements: Nanosecond transient absorption measurements were carried out using the SHG (532 nm) of an Nd:YAG laser (Spectra Physics, Quanta-Ray GCR-130, fwhm 6 ns) as excitation source. For the transient absorption spectra in the near-IR region (600–1600 nm), the monitoring light from a pulsed xenon lamp was detected with a Ge-avalanche photodiode (Hamamatsu Photonics, B2834).

Synthesis: Acetyleneferrocene was prepared from ferrocenecarbaldehyde according to the procedure described by Rodriguez.[28]

General Procedure for the Synthesis of Bis(ferrocenylacetylene)benzaldehydes 3a,b: After argon had been bubbled through triethylamine (125 mL) as solvent for 3 h, the aldehyde (1 equiv.), the catalysts $PdCl_2(PPh_3)_2$ (0.025 equiv.) and CuI (0.05 equiv.) and acetyl-

eneferrocene (6 equiv.) were added in this order. The reaction mixture was microwave-irradiated under argon in a microwave reactor focalized at 200 W during the indicated reaction time. After the irradiation, the orange-colored solution had completely turned brown. The solvent was removed under vacuum and the residue was purified by column chromatography on silica gel using toluene/hexane (7:3).

3,4-Bis(ferrocenylacetylene)benzaldehyde (3a): From 3,4-dibromobenzaldehyde, (100 mg, 0.38 mmol, 1 equiv.), $PdCl_2(PPh_3)_2$ (6.6 mg, 9.45 μmol, 0.025 equiv.), CuI (3.6 mg, 0.019 mmol, 0.05 equiv.) and ethynylferrocene (475 mg, 2.27 mmol, 6 equiv.). Reaction time 1.5 h, yield 93% (175 mg). IR-FT (KBr): $\tilde{\nu}$ = 2922, 2200, 1696, 1207, 813 cm^{-1}. ^1H NMR (200 MHz, $CDCl_3$): δ = 10.00 (s, 1 H), 7.99 (s, 1 H), 7.76 (d, J = 8.0 Hz, 1 H), 7.63 (d, J = 8.0 Hz, 1 H), 4.61 (s, 4 H), 4.33 (s, 4 H), 4.28 (s, 10 H) ppm. ^{13}C NMR (50 MHz, $CDCl_3$): δ = 191.0, 134.6, 133.2, 132.1, 131.8, 127.5, 127.4, 126.8, 126.7, 97.5, 94.1, 84.8, 83.8, 71.8, 71.7, 70.3, 70.2, 69.5, 69.2, 64.5, 64.2 ppm. UV/Vis (CH_2Cl_2): λ_{max}/nm (log ε) = 256.0 (4.43), 302.0 (4.39). $C_{31}H_{22}Fe_2O$ (522.2): calcd. C 71.26, H 4.24; found C 71.06, H 4.25. MALDI-TOF MS, m/z calculated for $C_{31}H_{22}OFe_2$ 522.04 (M^+), found 521.90 (M^+).

3,5-Bis(ferrocenylacetylene)benzaldehyde (3b): From 3,5-dibromobenzaldehyde, (100 mg, 0.38 mmol, 1 equiv.), $PdCl_2(PPh_3)_2$ (6.6 mg, 9.45 μmol, 0.025 equiv.), CuI (3.6 mg, 0.019 mmol, 0.05 equiv.) and ethynylferrocene (475 mg, 2.27 mmol, 6 equiv.). Reaction time 2 h, yield 184 mg (98%). IR-FT (KBr): $\tilde{\nu}$ = 2921, 2213, 1707, 1591, 1198, 802 cm^{-1}. ^1H NMR (200 MHz, $CDCl_3$): δ = 10.00 (s, 1 H), 7.90 (s, 2 H), 7.84 (s, 1 H), 4.54 (s, 4 H), 4.28 (s, 14 H) ppm. ^{13}C NMR (50 MHz, $CDCl_3$): δ = 191.1, 139.0, 136.6, 131.0, 129.0, 128.2, 125.5, 91.0, 83.8, 71.6, 70.1, 69.2, 64.2 ppm. UV/Vis (CH_2Cl_2): λ_{max}/nm (log ε) = 256.0 (4.46), 308.0 (4.37). MALDI-TOF MS, m/z calculated for $C_{31}H_{22}OFe_2$ 522.04 (M^+), found 521.74 (M^+). $C_{31}H_{22}OFe_2$ (522.2): C 71.26, H 4.24; found C 70.87, H 4.01.

General Procedure for the Synthesis of Pyrrolidino[60]fullerenes 4a,b. Method A: A mixture of C_{60} (1 equiv.), the corresponding aldehyde **3a**,**b** (2.5 equiv.) and *N*-methylglycine (5 equiv.) in dry toluene (250–300 mL for each mmol of C_{60}) was refluxed under argon during the indicated time. After cooling to room temperature, the crude product mixture was purified by column chromatography on silica gel using toluene/hexane (7:3). **Method B:** See method A, but use microwave irradiation (200 W) as source of energy.

2′-[3,4-Bis(ferrocenylacetylene)phenyl]-1′-methylpyrrolidino[3′,4′:1,2]-[60]fullerene (4a). Method A: Reaction time 5 h, yield 36%. **Method B:** Reaction time 1.5 h, yield 39%. IR-FT (KBr): $\tilde{\nu}$ = 2780, 2375, 2213, 1607, 1107, 839, 527 cm^{-1}. ^1H NMR (200 MHz, $CDCl_3$): δ = 7.72 (m, 1 H), 7.58 (m, 1 H), 7.54 (m, 1 H), 5.41 (d, J = 9.4 Hz, 1 H), 4.92 (s, 1 H), 4.58 (s, 2 H) 4.56 (s, 2 H), 4.27 (s, 4 H), 4.26 (s, 10 H), 2.83 (s, 3 H) ppm. ^{13}C NMR (50 MHz, $CDCl_3$): δ = 156.2, 154.0, 153.4, 153.0, 147.5, 146.8, 146.5, 146.4, 146.2, 145.8, 145.7, 145.5, 144.8, 144.6, 143.3, 143.2, 142.8, 142.3, 142.2, 141.9, 141.2, 140.4, 139.9, 137.2, 136.7, 136.1, 135.9, 132.4, 128.5, 126.3, 110.8, 93.3, 85.0, 84.9, 83.3, 82.6, 77.8, 71.8, 70.3, 69.3, 65.2, 62.0, 40.3 ppm. MALDI-TOF MS, m/z calculated for $C_{93}H_{27}Fe_2N$ 1269.08 (M^+), found 1269.00 (M^+), 720 (C_{60}). UV/Vis (CH_2Cl_2): λ_{max}/nm (log ε) = 255.0 (5.17), 431.0 (3.87).

2′-[3,5-Bis(ferrocenylacetylene)phenyl]-1′-methylpyrrolidino[3′,4′:1,2]-[60]fullerene (4b). Method A: Reaction time 8 h, yield 37%. **Method B:** Reaction time 2 h, yield 41%. IR (KBr): $\tilde{\nu}$ = 3101, 2927, 2903, 2780, 2213, 2201, 1531, 2374, 1078, 781, 692, 527 cm^{-1}. ^1H NMR (400 MHz, $CDCl_3$): δ = 7.85 (broad s, 2 H), 7.59 (t, J = 1.6 Hz, 1 H), 5.01 (d, J = 9.6 Hz, 1 H), 4.89 (s, 1 H), 4.51 (t, J = 1.6 Hz, 4 H), 4.28 (d, J = 9.5 Hz, 1 H), 4.24 (m, 14 H), 2.84 (s, 3 H) ppm. ^{13}C NMR (50 MHz, $CDCl_3$): δ = 156.2, 154.0, 153.3, 152.9, 147.5, 146.5, 146.4, 146.1, 146.0, 145.7, 145.5, 144.6, 142.8, 142.3, 142.2, 140.4, 137.8, 136.7, 135.9, 134.4, 131.4, 128.4, 124.8, 118.8, 89.8, 85.2, 83.2, 71.7, 70.2, 69.2, 64.9, 49.10 40.35 ppm. MALDI-TOF MS, m/z calculated for $C_{93}H_{27}Fe_2N$ 1269.08 (M^+), found 1269.00 (M^+), 720 (C_{60}). UV/Vis (CH_2Cl_2): λ_{max}/nm (log ε) = 255.0 (5.09), 431.0 (3.77).

General Procedure for the Synthesis of Hydrazones 5a,b: A solution containing 1 equiv. of the aldehyde, 1 equiv. of *p*-nitrophenylhydrazine and two drops of acetic acid in EtOH (150 mL for 1 mmol of aldehyde) was refluxed for the time indicated in each case. The mixture was then cooled to room temperature and then at 0 °C during 12 h. The solid was filtered and purified by recrystallization in EtOH.

3,4-Bis(ferrocenylacetylene)benzaldehyde *p*-Nitrophenylhydrazone (5a): Following the described procedure, from **3a** (100 mg, 0.19 mmol, 1 equiv.) and *p*-nitrophenylhydrazine (29.4 mg, 0.19 mmol, 1 equiv.). Reaction time 1 h, yield 112 mg (90%), m.p. >200 °C. IR-FT (KBr): $\tilde{\nu}$ = 3298, 2199, 1599, 1490, 1343, 1281, 1107 cm^{-1}. ^1H NMR (200 MHz, $CDCl_3$): δ = 8.20 (d, J = 9.0 Hz, 3 H), 7.75 (s, 2 H), 7.60 (d, J = 8.0 Hz, 1 H), 7.52 (d, J = 8.0 Hz, 1 H), 7.16 (d, J = 9.0 Hz, 2 H), 4.60 (s, 4 H), 4.31 (s, 4 H), 4.27 (s, 10 H) ppm. ^{13}C NMR (50 MHz, $CDCl_3$): δ = 149.4, 140.9, 140.2, 133.3, 132.3, 130.1, 127.1, 126.7, 126.4, 125.4, 112.1, 94.9, 93.3, 85.2, 84.7, 71.8, 70.4, 69.4, 69.3, 65.1, 65.0, 29.9 ppm. UV/Vis (CH_2Cl_2): λ_{max}/nm (log ε) = 301.0 (4.39), 410.0 (4.66). MALDI-TOF MS, m/z calculated for $C_{37}H_{27}N_3O_2Fe_2$ 657.08 (M^+), found 656.83 (M^+). $C_{37}H_{27}N_3O_2Fe_2$ (657.32): C 67.57, H 4.14, N 6.39; found C 67.23, H 4.35, N 6.28.

3,5-Bis(ferrocenylacetylene)benzaldehyde *p*-Nitrophenylhydrazone (5b): Following the described procedure, from **3b** (100 mg, 0.19 mmol, 1 equiv.) and *p*-nitrophenylhydrazine (29.4 mg, 0.19 mmol, 1 equiv.). Reaction time 0.5 h, yield 104 mg (83%), m.p. 163 °C. IR-FT (KBr): $\tilde{\nu}$ = 3278, 2215, 1595, 1498, 1343, 1262, 1107 cm^{-1}. ^1H NMR (200 MHz, $CDCl_3$): δ = 8.22 (d, J = 9.0 Hz, 2 H), 8.11 (s, 1 H), 7.71 (s, 2 H), 7.61 (s, 1 H), 7.49 (s, 1 H), 7.19 (d, J = 9.0 Hz, 2 H), 4.54 (s, 4 H), 4.27 (s, 14 H) ppm. ^{13}C NMR (125 MHz, [D_6]DMSO): δ = 150.4, 139.9, 138.7, 135.9, 133.4, 127.9, 126.1, 124.1, 111.7, 90.1, 84.3, 71.3, 69.9, 69.2, 63.9 ppm. UV/Vis (CH_2Cl_2): λ_{max}/nm (log ε) = 306.0 (4.50), 394.0 (4.53). MALDI-TOF MS, m/z calculated for $C_{37}H_{27}N_3O_2Fe_2$ 657.08 (M^+), found 656.63 (M^+). $C_{37}H_{27}N_3O_2Fe_2$ (657.32): C 67.57, H 4.14, N 6.39; found C 66.89, H 4.28, N 6.10.

General Procedure for the Preparation of 2-Pyrazolino[60]fullerenes 6a,b. Method A: To a solution containing 0.06 mmol of the corresponding hydrazone in 10 mL of dry $CHCl_3$ under argon was added 0.005 mL of anhydrous pyridine. The mixture was then cooled to 0 °C and 0.12 mmol of *N*-chlorosuccinimide (NCS) were added. After stirring for 30 min at 0 °C and 60 min at room temperature, a solution containing 0.06 mmol of C_{60} and 0.15 mmol of triethylamine in 45 mL of dry toluene was added. The mixture was stirred at room temperature during the specified reaction time. The crude product was purified by flash column chromatography over silica gel using toluene/hexane (7:3). **Method B:** See method A, but use microwave irradiation (200 W) as source of energy.

2′-[3,4-Bis(ferrocenylacetylene)phenyl]-1′-(*p*-nitrophenyl)-2-pyrazolino-[4′,5′:1,2][60]fullerene (6a): Method A: Reaction time 3 h, yield 27%. **Method B:** Reaction time 1 h, yield 27%. IR (KBr): $\tilde{\nu}$ = 3090, 2202, 1589, 1543, 1511, 1381, 1042, 526 cm^{-1}. ^1H NMR (200 MHz, $CDCl_3$): δ = 8.38 (s, 1 H), 8.36 (d, J = 9.0 Hz, 2 H), 8.29 (d, J = 9.0 Hz, 2 H), 8.11 (d, J = 8.2 Hz, 1 H), 7.62 (d, J = 8.2 Hz, 1 H),

4.59 (s, 4 H), 4.30 (s, 4 H), 4.25 (s, 10 H) ppm. MALDI-TOF MS, *m/z* calculated for $C_{97}H_{25}N_3O_2Fe_2$ 1375.10 (M^+), found 1375.14 (M^+), 720 (C_{60}). UV/Vis (CH_2Cl_2): λ_{max}/nm (log ε) = 255.0 (5.15), 320.0 (4.84).

2′-[3,5-Bis(ferrocenylacetylene)phenyl]-1′-(*p*-nitrophenyl)-2-pyrazolino-[4′,5′:1,2][60]fullerene (6b). Method A: Reaction time 3 h, yield 17%. **Method B:** Reaction time 1.5 h, yield 25%. IR (KBr): $\tilde{\nu}$ = 3094, 2917, 2213, 1590, 1512, 1314, 852, 527 cm^{-1}. ^1H NMR (400 MHz, $CDCl_3$): δ = 8.36 (d, J = 9.2 Hz, 2 H), 8.28 (d, J = 9.2 Hz, 2 H), 8.21 (d, J = 1.4 Hz, 2 H), 7.74 (t, J = 1.6 Hz, 1 H), 4.51 (t, J = 1.6 Hz, 4 H), 4.26 (t, J = 1.8 Hz, 4 H), 4.23 (s, 10 H) ppm. MALDI-TOF MS, *m/z* calculated for $C_{97}H_{25}N_3O_2Fe_2$ 1375.07, found 1375.14 (M^+), 720 (C_{60}). UV/Vis (CH_2Cl_2): λ_{max}/nm (log ε) = 255.0 (5.14), 316.0 (4.78).

Supporting Information (see also the footnote on the first page of this article): The characterization data including IR-FT, ^1H NMR, ^{13}C NMR, and MALDITOF-MS of new compounds.

Acknowledgments

Financial support from the Spanish Ministerio de Educación y Ciencia (MEC), Federación Española de Enfermedades Raras (FEDER) funds (Project CTQ2007-63363/PPQ and Consolider project HOPE (CSD2007-00007) and the Junta de Comunidades de Castilla-La Mancha (Project PCI08-038) is gratefully acknowledged. This work was also supported by the Tohoku University (21st Century Center of Excellence Program "Giant Molecules and Complex Systems").

[1] a) J. L. Segura, N. Martín, D. M. Guldi, *Chem. Soc. Rev.* **2005**, *34*, 31–47; b) Roncali, *J. Chem. Soc. Rev.* **2005**, *34*, 483–495; c) T. M. Figueira-Duarte, A. Gégout, J.-F. Nierengarten, *Chem. Commun.* **2007**, 109–119.

[2] L. Echegoyen, L. E. Echegoyen, *Acc. Chem. Res.* **1998**, *31*, 593–601.

[3] a) H. Imahori, S. Fukuzumi, *Adv. Funct. Mater.* **2004**, *14*, 525–536; b) P. A. Liddell, J. P. Sumida, A. N. Macpherson, L. Noss, G. R. Seely, K. N. Clark, A. L. Moore, T. A. Moore, D. Gust, *Photochem. Photobiol.* **1994**, *60*, 537–541; c) H. Imahori, S. Cardoso, D. Tatman, S. Lin, L. Noss, G. R. Seely, L. Sereno, J. C. deSilber, T. A. Moore, A. L. Moore, D. Gust, *Photochem. Photobiol.* **1995**, *62*, 1009–1014; d) N. Watanabe, N. Kihara, Y. Furusho, T. Takata, Y. Araki, O. Ito, *Angew. Chem. Int. Ed.* **2003**, *42*, 681–683.

[4] a) A. Gouloumis, S.-G. Liu, A. Sastre, P. Vázquez, L. Echegoyen, T. Torres, *Chem. Eur. J.* **2000**, *6*, 3600–3607; b) A. de la Escosura, M. V. Martínez-Díaz, D. M. Guldi, T. Torres, *J. Am. Chem. Soc.* **2006**, *128*, 4112–4118.

[5] a) J. N. Clifford, G. Accorsi, F. Cardinali, J.-F. Nierengarten, N. Armaroli, *C. R. Chim.* **2006**, *9*, 1005–1013; b) K. Lee, H. Song, B. Kim, J. T. Park, S. Park, M.-G. Choi, *J. Am. Chem. Soc.* **2002**, *124*, 2872–2873.

[6] a) E. M. Pérez, M. Sierra, L. Sánchez, M. R. Torres, R. Viruela, P. M. Viruela, E. Ortí, N. Martín, *Angew. Chem. Int. Ed.* **2007**, *46*, 1847–1851; b) E. M. Priego, L. Sánchez, M. A. Herranz, N. Martín, R. Viruela, E. Orti, *Org. Biomol. Chem.* **2007**, *5*, 1201–1209; c) M. C. Díaz, B. M. Illescas, N. Martín, I. F. Perepichka, M. R. Bryce, E. Levillain, R. Viruela, E. Ortí, *Chem. Eur. J.* **2006**, *12*, 2709–2721.

[7] a) M. Maggini, G. Scorrano, M. Prato, *J. Am. Chem. Soc.* **1993**, *115*, 9798–9799; b) M. Prato, M. Maggini, C. Giacometti, G. Scorrano, G. Sandona, G. Farnia, *Tetrahedron* **1996**, *52*, 5221–5234; c) F. D'Souza, M. E. Zandler, P. M. Smith, G. R. Deviprasad, K. Arakady, M. Fujitsuka, O. Ito, *J. Phys. Chem. A* **2002**, *106*, 649–656; d) F. D'Souza, M. E. Zandler, P. M. Smith, G. R. Deviprasad, K. Arakady, M. Fujitsuka, O. Ito, *J. Org. Chem.* **2002**, *67*, 9122–9129; e) M. Fujitsuka, O. Ito, H. Imahori, K. Yamada, H. Yamada, Y. Sakata, *Chem. Lett.* **1999**, 721–722; f) H. Imahori, K. Tamaki, D. M. Guldi, C. Luo, M. Fujitsuka, O. Ito, Y. Sakata, S. Fukuzumi, *J. Am. Chem. Soc.* **2001**, *123*, 2607–2617; g) A. Polese, S. Mondini, A. Bianco, C. Toniolo, G. Scorrano, D. M. Guldi, M. Maggini, *J. Am. Chem. Soc.* **1999**, *121*, 3446–3452.

[8] a) J.-F. Nierengarten, N. Armaroli, G. Accorsi, Y. Rio, J.-F. Eckert, *Chem. Eur. J.* **2003**, *9*, 37–41; b) G. Accorsi, N. Armaroli, J.-F. Eckert, J.-F. Nierengarten, *Tetrahedron Lett.* **2002**, *43*, 65–68; c) J. L. Segura, R. Gómez, N. Martín, C. Luo, A. Swartz, D. M. Guldi, *Chem. Commun.* **2001**, 707–708; d) M. Schwell, N. K. Wachter, J. R. Rice, J. P. Galaup, S. Leach, R. Taylor, R. V. Bensasson, *Chem. Phys. Lett.* **2001**, *339*, 29–35; e) D. M. Guldi, A. Swartz, C. Luo, R. Gomez, J. L. Segura, N. Martin, *J. Am. Chem. Soc.* **2002**, *124*, 10875–10886; f) N. Armaroli, G. Accorsi, J. N. Clifford, J.-F. Eckert, J.-F. Nierengarten, *Chem. Asian J.* **2006**, *1*, 564–574.

[9] L. Perez, J. C. García-Martinez, E. Diez-Barra, P. Atienzar, H. Garcia, J. Rodriguez-Lopez, F. Langa, *Chem. Eur. J.* **2006**, *12*, 5149–5157.

[10] L. Perez, M. E. El-Khouly, P. de la Cruz, Y. Araki, O. Ito, F. Langa, *Eur. J. Org. Chem.* **2007**, 2175–2185.

[11] L. Sánchez, M. A. Herranz, N. Martín, *J. Mater. Chem.* **2005**, *15*, 1409–1421, and references therein.

[12] a) J.-F. Nierengarten, *New J. Chem.* **2004**, *28*, 1177–1191; b) N. Martín, *Chem. Commun.* **2006**, 2093–2104; c) J. N. Clifford, A. Gégout, S. Zhang, R. Pereira de Freitas, M. Urbani, M. Holler, P. Ceroni, J.-F. Nierengarten, N. Armaroli, *Eur. J. Org. Chem.* **2007**, 5899–5908.

[13] a) J.-F. Nierengarten, T. Gu, G. Hadziioannou, D. Tsamouras, V. Krasnikov, *Helv. Chim. Acta* **2004**, *87*, 2948–2966; b) C. Atienza, N. Martín, M. Wielopolski, N. Haworth, T. Clark, D. M. Guldi, *Chem. Commun.* **2006**, 3202–3204; c) K. Tashiro, A. Sato, T. Yuzawa, T. Aida, K. Yamanaka, M. Fujitsuka, O. Ito, *Chem. Lett.* **2006**, 518–519; d) N. Zhou, L. Wang, D. W. Thompson, Y. Zhao, *Tetrahedron Lett.* **2007**, *48*, 3563–3567; e) T. M. Figueira-Duarte, Y. Rio, A. Listorti, B. Delavaux-Nicot, M. Holler, F. Marchioni, P. Ceroni, N. Armaroli, J.-F. Nierengarten, *New J. Chem.* **2008**, *32*, 54–64.

[14] J. G. Rodríguez, A. Oñate, R. M. Martín-Villamil, I. Fonseca, *J. Organomet. Chem.* **1996**, *513*, 71–76.

[15] K. Sonogashira, *Handbook of Organopalladium Chemistry for Organic Synthesis* (Ed.: E. Negishi), Wiley-Interscience, **2002**, p. 493.

[16] a) P. Nilsson, K. Olofsson, M. Larhed, *Top. Curr. Chem.* **2006**, *266*, 103–144; b) A. Gouloumis, F. Oswald, M. E. El-Khouly, F. Langa, Y. Araki, O. Ito, *Eur. J. Org. Chem.* **2006**, 2344–2351.

[17] Focused microwave oven from CEM Discovery Ltd.

[18] M. Prato, M. Maggini, *Acc. Chem. Res.* **1998**, *31*, 519–526.

[19] A. de la Hoz, A. Diaz-Ortiz, A. Moreno, F. Langa, *Eur. J. Org. Chem.* **2000**, 3659–3673.

[20] a) P. de la Cruz, A. de la Hoz, F. Langa, B. Illescas, N. Martín, *Tetrahedron* **1997**, *53*, 2599–2608; b) F. Langa, P. de la Cruz, E. Espíldora, J. J. García, M. C. Pérez, A. de la Hoz, *Carbon* **2000**, *38*, 1641–1646.

[21] a) P. de la Cruz, A. Díaz-Ortiz, J. J. García, M. J. Gómez-Escalonilla, A. de la Hoz, F. Langa, *Tetrahedron Lett.* **1999**, *40*, 1587–1590; b) F. Langa, P. de la Cruz, E. Espíldora, A. de la Hoz, J. L. Bourdelande, L. Sánchez, N. Martín, *J. Org. Chem.* **2001**, *66*, 5033–5041; c) F. Langa, M. J. Gómez-Escalonilla, E. Diez-Barra, J. C. García-Martínez, A. de la Hoz, J. Rodríguez-López, A. González-Cortes, V. López-Arza, *Tetrahedron Lett.* **2001**, *42*, 3435–3438; d) J. L. Delgado, P. de la Cruz, V. López-Arza, F. Langa, D. B. Kimball, M. M. Haley, *J. Org. Chem.* **2004**, *69*, 2661–2666; e) F. Langa, M. J. Gómez-Escalonilla, J.-M. Rueff, T. M. Figueira Duarte, J.-F. Nierengarten, V. Palermo, P. Samorì, Y. Rio, G. Accorsi, N. Armaroli, *Chem. Eur. J.* **2005**, *11*, 4405–4415.

[22] a) P. de la Cruz, A. de la Hoz, L. M. Font, F. Langa, M. C. Pérez-Rodríguez, *Tetrahedron Lett.* **1998**, *39*, 6053–6056; b) F. Ajamaa, T. M. Figueira-Duarte, C. Bourgogne, M. Holler, P. W. Fowler, J.-F. Nierengarten, *Eur. J. Org. Chem.* **2005**, 3766–3774.

[23] a) S. Yoshimoto, A. Saito, E. Tsutsumi, F. D'Souza, O. Ito, K. Itaya, *Langmuir* **2004**, *20*, 11046–11052; b) F. D'Souza, M. E. Zandler, P. M. Smith, G. R. Deviprasad, K. Arkady, M. Fujitsuka, O. Ito, *J. Phys. Chem. A* **2002**, *106*, 649–656.

[24] a) F. Langa, P. de la Cruz, J. L. Delgado, M. J. Gómez-Escalonilla, A. González-Cortés, A. de la Hoz, V. López-Arza, *New J. Chem.* **2002**, *26*, 76–80; b) E. Espildora, J. L. Delgado, P. de la Cruz, A. de la Hoz, V. López-Arza, F. Langa, *Tetrahedron* **2002**, *58*, 5821–5826.

[25] a) R. A. Marcus, *J. Chem. Phys.* **1956**, *24*, 966–978; b) R. A. Marcus, *J. Chem. Phys.* **1957**, *26*, 867–871; c) R. A. Marcus, *J. Chem. Phys.* **1957**, *26*, 872–877; d) R. A. Marcus, *J. Chem. Phys.* **1965**, *43*, 679–701; e) R. A. Marcus, N. Sutin, *Biochim. Biophys. Acta* **1985**, *811*, 265–322.

[26] H. Imahori, K. Hagiwara, T. Akiyama, M. Aoki, S. Taniguchi, T. Okada, M. Shirakawa, Y. Sakata, *Chem. Phys. Lett.* **1996**, *263*, 545–550.

[27] a) Y. Araki, Y. Yasumura, O. Ito, *J. Phys. Chem. B* **2005**, *109*, 9843–9848; b) M. Otake, M. Itou, Y. Araki, O. Ito, H. Kido, *Inorg. Chem.* **2005**, *44*, 8581–8586.

[28] J. G. Rodriguez, A. Oñate, R. M. Martin-Villamil, I. Fonseca, *J. Organomet. Chem.* **1996**, *513*, 71–76.

Received: April 1, 2008
Published Online: June 3, 2008

